

Structural, Electronic, and Vibrational Characterization of Fe–HNO Porphyrinates by Density Functional Theory

Douglas P. Linder and Kenton R. Rodgers*

Department of Chemistry, Biochemistry, and Molecular Biology, North Dakota State University, Fargo, North Dakota 58105-5516

Received March 31, 2005

A recent report of the structural and vibrational properties of heme-bound HNO in myoglobin, MbHNO, revealed a long Fe–N_{HNO} bond with the hydrogen atom bonded to the coordinated N atom. The Fe–N(H)–O moiety was reported to exhibit an unusually high Fe–N_{HNO} stretching frequency relative to those of the corresponding {FeNO}⁶ and {FeNO}⁷ porphyrinates, despite the Fe–N_{HNO} bond being longer than either of its Fe–N_{NO} counterparts. Herein, we present results from density functional theory calculations of an active site model of MbHNO that support the previous assignment and clarify this seemingly contradictory result. The results are consistent with the experimental evidence for a ground-state Fe–N(H)–O structure having a long Fe–N_{HNO} bond and a uniquely high $\nu_{\text{Fe–N(HNO)}}$ frequency. This high frequency is the result of the correspondingly low reduced mass of the normal mode, which is largely attributable to significant motion of the N-bound hydrogen atom. Additionally, the calculations show the Fe–N(H)O bonding in this complex to be remarkably insensitive to whether the HNO and ImH ligand planes are parallel or perpendicular. This is attributed to insensitivities of the Fe–L_{axial} characters of molecular orbitals to the relative HNO and ImH orientation in both the parallel and perpendicular conformers.

Introduction

Interactions of nitric oxide (NO) with heme proteins and enzymes play pivotal roles in both prokaryotes and eukaryotes.^{1,2} In recent years, a newly recognized player in the biological chemistry of NO species, HNO (nitrosyl hydride or nitroxyl), has captured the interest of the NO community.^{3–5} HNO intermediates have been proposed in the catalytic cycles of NO synthase⁶ as well as the nitrite⁷ and NO reductases.⁸ As evidence of the plausibility of these inter-

mediates, an unusually stable HNO adduct of myoglobin, MbHNO, has been isolated and characterized.^{4,5,9,10} Although, by virtue of its stability, this complex may not be an accurate mimic of reactive intermediates, it certainly provides a platform for characterization of the interplay between structure and bonding in the heme FeHNO moiety. A very recent report of XANES, EXAFS, and resonance Raman (rR) results from MbHNO has shed considerable light on its structural and vibrational properties.¹⁰ That study revealed peculiarities of MbHNO that warrant further examination. For example, the reported Fe–N_{HNO} vibrational stretching frequency of 651 cm⁻¹ is significantly higher than its counterparts in Mb{FeNO}⁶ (595 cm⁻¹) and Mb{FeNO}⁷ (551 cm⁻¹), despite the reported Fe–N_{HNO} bond length of 1.82 Å being significantly longer than the respective Fe–N_{NO} bond lengths of 1.68 and 1.76 Å. Additionally, the rR spectrum of MbHNO contains an unassigned band at 1408

* To whom correspondence should be addressed. E-mail: kent.rodders@ndsu.edu. Tel: (701) 231-8746. Fax: (701) 231-8831.

- (1) (a) Culotta, E.; Koshland, D. E., Jr. *Science* **1992**, *258*, 1862–1865. (b) Cooper, C. E. *Biochim. Biophys. Acta* **1999**, *1411*, 290–309. (c) *Methods in Nitric Oxide Research*; Feelisch, M., Stamler, J. S., Eds.; Wiley: Chichester, U.K., 1996.
- (2) McCleverty, J. A. *Chem. Rev.* **2004**, *104*, 403–418.
- (3) (a) Wilson, E. K. *Chem. Eng. News* **2004**, *82* (10), 39–44. (b) Paolocci, N.; Katori, T.; Champion, H. C.; St. John, M. E.; Miranda, K. M.; Fukuto, J. M.; Wink, D. A. *Proc. Natl. Acad. Sci. U.S.A.* **2003**, *100*, 5537–5542.
- (4) (a) Farmer, P. J.; Sulc, F. J. *J. Inorg. Biochem.* **2005**, *99*, 166–184. (b) Miranda, K. *Coord. Chem. Rev.* **2005**, *249*, 433–455.
- (5) Sulc, F.; Fleischer, E.; Farmer, P. J.; Ma, D.; LaMar, G. N. *J. Biol. Inorg. Chem.* **2003**, *8*, 348–352.
- (6) Rusche, K. M.; Spiering, M. M.; Marletta, M. A. *Biochemistry* **1998**, *37*, 15503–15512.
- (7) Einsle, O.; Messerschmidt, A.; Huber, R.; Kroneck, P. M. H.; Neese, F. *J. Am. Chem. Soc.* **2002**, *124*, 11737–11745.

(8) Averill, B. A. *Chem. Rev.* **1996**, *96*, 2951–2964.

- (9) (a) Lin, R.; Farmer, P. J. *J. Am. Chem. Soc.* **2000**, *122*, 2393–2394. (b) Sulc, F.; Immoos, C. E.; Pervitski, D.; Farmer, P. J. *J. Am. Chem. Soc.* **2004**, *126*, 1096–1101.
- (10) Immoos, C. E.; Sulc, F.; Farmer, P. J.; Czarnecki, K.; Bocian, D. F.; Levina, A.; Aitken, J. B.; Armstrong, R. S.; Lay, P. A. *J. Am. Chem. Soc.* **2005**, *127*, 814–815.

cm^{-1} that shifts 5 cm^{-1} to lower frequency upon H^{15}NO substitution.

Herein we present the results of density functional theory (DFT) calculations of the iron porphinate [$\text{FeP}(\text{ImH})\text{HNO}$] as a model of the heme in MbHNO. The calculated Fe–N(H)–O bonding parameters in this model are compared and contrasted with those of MbHNO in order to gain insight into the relationships between the structural, electronic, and vibrational properties of this heme protein complex.

Methods

The quantum mechanical DFT calculations were performed with the B3LYP and BLYP methods as implemented in *Gaussian 03*.¹¹ The 6-31G(d) or 6-311G(2d,2p) basis sets were used on H, C, N, and O, with the all-electron 6-311+G basis set used on Fe. Full geometry optimizations and force-constant calculations were performed on all systems, using an ultrafine integration grid and no symmetry constraints. The energy differences listed are electronic energy differences, and no scaling factors are used in the reported vibrational frequencies. In general, restricted singlet electronic state calculations were performed for the [$\text{FeP}(\text{ImH})\text{HNO}$] species because experimental results indicate MbHNO is diamagnetic.^{4,5} No low-lying triplet states were located by our calculations.

Results and Discussion

The EXAFS structure of the heme in MbHNO indicates Fe–N_{HNO} coordination,¹⁰ with the H atom bonded to the N atom.^{4,5} Consistent with this result, geometry optimizations performed at the B3LYP/6-31G(d) level of theory indicate that a N(H) coordinated structure is, by far, the lowest energy [$\text{FeP}(\text{ImH})\text{HNO}$] isomer, as shown in Figure 1.¹² Other identified isomers include two Fe–O–NH complexes (2 and 3 in Figure 1) that are >50 kJ/mol higher in energy, two Fe–N–OH systems (4 and 5 in Figure 1) that are >90 kJ/mol higher in energy, and an Fe–OH–N isomer (6 in Figure 1) that is over 250 kJ/mol higher in energy. The experimental structure of MbHNO also indicates that the (H)NO ligand plane is roughly perpendicular (\perp) to the proximal ImH.^{4,5,10} Large basis set [6-311G(2d,2p)] B3LYP and BLYP calculations minimize with the HNO parallel (\parallel) and perpendicular (\perp) to the proximal imidazole ring, respectively, with the ligand planes oriented between the pyrrole N atoms of the porphyrin (Figure 2). The DFT methods predict that these

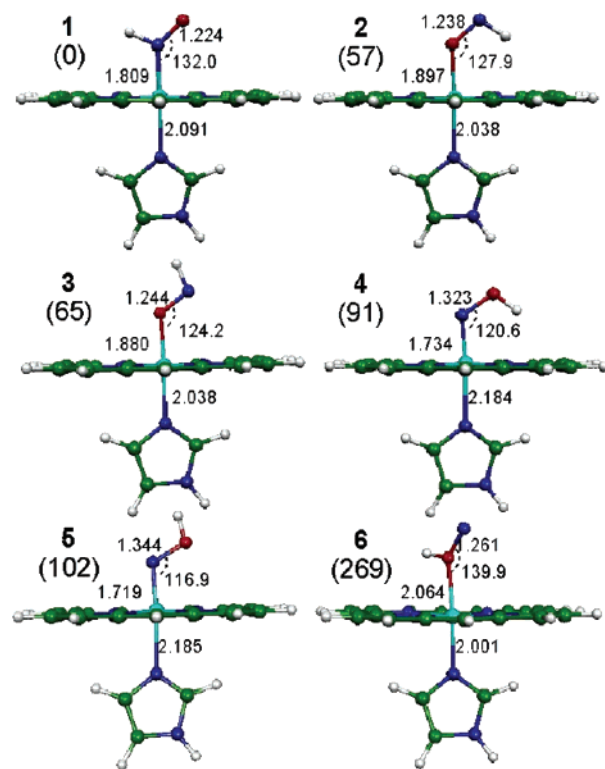


Figure 1. B3LYP/6-31G(d)-optimized isomers of [$\text{FeP}(\text{ImH})\text{HNO}$]. Energy values (in parentheses) are in kilojoules per mole. Colors: N, blue; O, red; H, white; C, green. Bond lengths are in angstroms, and angles are in degrees.

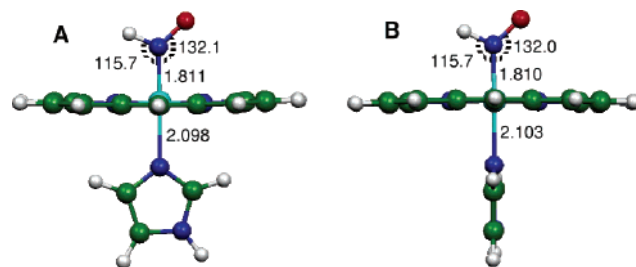


Figure 2. B3LYP/6-311G(2d,2p)-optimized [$\text{FeP}(\text{ImH})\text{HNO}$] structures showing the (A) parallel and (B) perpendicular orientations of the HNO and ImH planes. Bond lengths are in angstroms, and angles are in degrees.

structures are very close in energy, with the BLYP method predicting \perp to be more stable by 0.7 kJ/mol and B3LYP predicting \parallel to be more stable by 0.2 kJ/mol. Regardless of the DFT method used, there appears to be very little intrinsic stabilization of either HNO orientation in the gas phase. Unrestricted singlet-state calculations did not lower the energies of these structures. Moreover, the Fe–N(H)–O bond distances and angles are calculated to be essentially the same in both conformers (Table 1). These energetic and structural similarities suggest that Fe–N(H)–O bonding is not influenced to a significant extent by the relative orientations of the HNO and ImH ligands. Barring any potentially offsetting electronic effects of changes in axial ligand orientations on the structure, this would lead one to predict that Fe–N(H)O and Fe–ImH π bonding are uncoupled in these two complexes. In other words, molecular orbitals (MOs) having both Fe–ImH and Fe–N(H)O π character would not be expected because they would have to be distinct

(11) Frisch, M. J.; Trucks, G. W.; Schlegel, H. B.; Scuseria, G. E.; Robb, M. A.; Cheeseman, J. R.; Montgomery, J. A., Jr.; Vren, T.; Kudin, K. N.; Burant, J. C.; Millam, J. M.; Iyengar, S. S.; Tomasi, J.; Barone, V.; Mennucci, M.; Cossi, M.; Scalmani, G.; Rega, N.; Petersson, G. A.; Nakatsuji, H.; Hada, M.; Ehara, M.; Toyota, K.; Fukuda, R.; Hasegawa, J.; Ishida, M.; Nakajima, T.; Honda, Y.; Kitao, O.; Nakai, H.; Klene, M.; Li, X.; Knox, J. E.; Hratchian, H. P.; Cross, J. B.; Adamo, C.; Jaramillo, J.; Gomperts, R.; Stratmann, R. E.; Yazyev, O.; Austin, A. J.; Cammi, R.; Pomelli, C.; Ochterski, J. W.; Ayala, P. Y.; Morokuma, K.; Voth, G. A.; Salvador, P.; Dannenberg, J. J.; Zakrzewski, V. G.; Dapprich, S.; Daniels, A. D.; Strain, M. C.; Farkas, O.; Malick, D. K.; Rabuck, A. D.; Raghavachari, K.; Foresman, J. B.; Ortiz, V. J.; Cui, Q.; Baboul, A. G.; Clifford, S.; Cioslowski, J.; Stefanov, B. B.; Liu, G.; Liashenko, A.; Piskorz, P.; Komaromi, I.; Martin, R. L.; Fox, D. J.; Keith, T.; Al-Laham, M. A.; Peng, C. Y.; Nanayakkara, A.; Challacombe, M.; Gill, P. M. W.; Johnson, B.; Chen, W.; Wong, M. W.; Gonzalez, C.; Pople, J. A. *Gaussian 03*, Revision B.05; Gaussian, Inc.: Pittsburgh, PA, 2003.

(12) All figures were produced with the program MOLEKEL, version 4.2. <http://www.cscs.ch/molekel/>. Portman, S.; Luthi, H. P. *Chimia* **2000**, *54*, 766–770.

Table 1. Selected Structural and Vibrational Parameters for FeHNO Porphyrinates

complex	bond lengths (Å) and angles (deg)					vibrational stretching and bending frequencies (cm ⁻¹)						ΔE (kJ/mol)
	Fe–N(XNO)	N–O	Fe–ImH	N–H	\angle FeNO	N–H	N–O	Fe–N(XNO)	HNO(ip)	HNO(oop)	FeNO	
MbHNO ^a	1.82(2)	1.24(1)	2.09(3)		131(6)		1385	651	1408 ^b			
MbH ¹⁵ NO									–30	–15	–5 ^b	
HNO ^c		1.211		1.063			2685	1565		1500		
						B3LYP/6-311G(2d,2p) Method						
HNO(<i>S</i> = 0)		1.201		1.063			2848	1655		1573		
[FeP(ImH)HNO]	1.811	1.217	2.098	1.042	132.1	3123	1544	619	1515	862	449	0
[FeP(ImH)HNO] \perp	1.810	1.217	2.103	1.042	132.0	3121	1543	615	1513	861	448	0.2
						BLYP/6-311G(2d,2p) Method						
HNO(<i>S</i> = 0)		1.218		1.082		2625	1559		1489			
[FeP(ImH)HNO]	1.802	1.243	2.146	1.049	131.8	3008	1417	634	1430	814	450	0.7
[FeP(ImH)HNO] \perp	1.802	1.243	2.144	1.049	131.8	3008	1416	631	1427	815	448	0
[FeP(ImH) ² HNO] \perp						–808	1	–39	–347	–98	0	
[FeP(ImH)H ¹⁵ NO] \perp						–6	–24	–15	–6	–11	–2	
[FeP(ImH)HN ¹⁸ O] \perp						0	–35	0	–2	–1	–5	
						B3LYP/6-31G(d) Method						
[FeP(ImH)NO] [–] (<i>S</i> = 1)	1.765	1.181	2.163			140.3	1777	561			438	0
[FeP(ImH)NO] [–] (<i>S</i> = 0)	1.814	1.215	2.419			120.3	1578	607			431	4.5
[FeP(ImH)NO] [–] (<i>S</i> = 1) ^d	1.735	1.208	2.366			140.1	1612	575			452	

^a MbHNO.¹⁰ ^b This mode is unassigned in the rR spectra. ^c Bond lengths¹⁴ and vibrational frequencies.¹⁵ ^d BLYP/6-31G(d) method.

for the || and \perp conformers and would likely exert differential effects on the stabilities of the complexes.

As a means of testing this hypothesis, all filled MOs of both the || and \perp [FeP(ImH)HNO] conformers were examined and subjected to a side-by-side comparison. Figure S1 in the Supporting Information shows all of the filled Kohn–Sham orbitals having Fe–L_{axial} character for the \perp and || conformers (the only exception is MO 104, which exhibits no Fe–L_{axial} character but comparable porphyrin–ImH interactions in the two conformers). The orbitals illustrate two interesting generalities. First, none of these MOs have both Fe–N(H)O and Fe–ImH π character. In fact, none of the occupied MOs have Fe–ImH π character. Localization of Fe–L_{axial} π bonding to the HNO side of the porphyrin, as illustrated in MOs 116 and 84, and the striking similarity of the Fe–L_{axial} characters of these MOs for the \perp and || conformers suggest that the π contributions to Fe–N(H)–O bonding are independent of whether the HNO and ImH orientations are parallel or perpendicular. The second generality is that the only MOs having both Fe–N(H)O and Fe–ImH character (MOs 114, 101, 98, 97, 88, 81, 80, 74, and 57) are either σ bonding or σ antibonding with respect to the Fe–L_{axial} bonds. Moreover, the characters of the respective orbitals for the \perp and || forms are also strikingly similar. In other words, the contributions of these σ MOs to the Fe–N(H)–O and Fe–ImH bonding appear to be independent of whether the axial ligand planes are parallel or perpendicular. A similar lack of orientational influence on energy and FeNO bonding has been reported for the analogous {FeNO}⁷ porphyrinate, [FeP(ImH)NO].¹³

The MbHNO EXAFS structure reveals that the FeNO plane is nearly parallel to a vector connecting opposing pyrrole N atoms and perpendicular to the proximal ImH ring (\perp'). Both the BLYP/6-311G(2d,2p) and B3LYP/6-31G(d) methods predict the analogous [FeP(ImH)HNO] structure to have an essentially planar porphyrin ligand, as observed in

the \perp and || structures, but to be higher in energy than the ground-state structure (BLYP; $\Delta E = 3.4$ kJ/mol). Vibrational frequency calculations show that the structures from both methods occur at second-order saddle points, where the HNO and ImH ligands undergo torsional motion about their Fe–N bonds. Further geometry optimizations using the second derivative matrix from the frequency calculations of the aforementioned \perp' structures yielded structures with their axial ligand planes oriented between the pyrrole N atoms, consistent with these structures being the intrinsically most stable. Thus, in addition to the || and \perp axial ligand conformers being the most stable and nearly isoenergetic, the barrier to rotation of the axial ligands about their Fe–N bonds appears to be only a few kilojoules per mole. This suggests that the \perp' axial ligand conformation in MbHNO is stabilized through influences of the protein structure, consistent with the earlier conclusion for the corresponding {FeNO}⁷ complex, [FeP(ImH)NO].¹³

Because the HNO and ImH planes are perpendicular in MbHNO,^{5,10} we have based our comparisons of the FeNO bonding properties in these complexes on that orientation. The experimental structural and vibrational parameters for MbHNO and those calculated in this study for [FeP(ImH)HNO] and HNO are summarized in Table 1.^{10,14,15} Overall, both the B3LYP and BLYP methods yield [FeP(ImH)HNO] structures that are in good agreement with the EXAFS structure for MbHNO, with neither method providing a clear-cut best structure. The high-energy isomers shown in Figure 1 all have bond lengths and/or bond angles that differ significantly from those of MbHNO, consistent with conclusions, based on NMR⁵ and EXAFS¹⁰ studies, that the HNO ligand coordinates through its N(H) moiety. Although there are minor differences between the absolute bonding parameters obtained from the B3LYP and BLYP methods (i.e.,

(14) Dalby, F. W. *Can. J. Phys.* **1958**, *36*, 1336.

(15) (a) Clough, P. N.; Thrush, B. A.; Ramsay, D. A.; Stamper, J. G. *Chem. Phys. Lett.* **1973**, *23*, 155–156. (b) Johns, J. W. C.; McKellar, A. R. W. *J. Chem. Phys.* **1977**, *66*, 1217–1224.

(13) Patchkovskii, S.; Ziegler, T. *Inorg. Chem.* **2000**, *39*, 5354–5364.

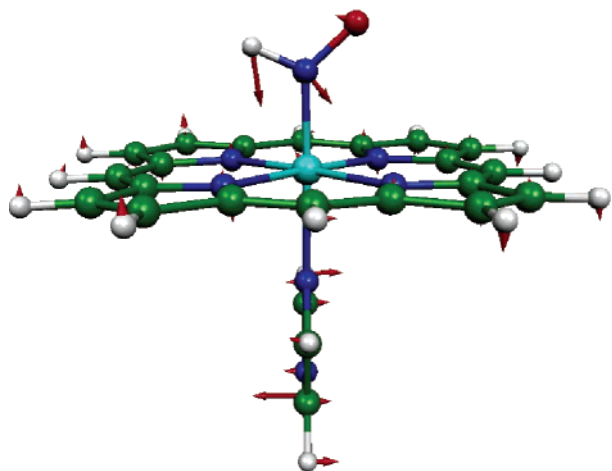


Figure 3. BLYP-calculated normal-mode eigenvector for $\nu_{\text{Fe-N(HNO)}}$.

BLYP predicts $R_{\text{N-O}}$ and $R_{\text{Fe-N(ImH)}}$ to be 0.026 and 0.041 Å longer, respectively, than those of B3LYP, these methods provide optimized structures that are otherwise very similar.

Although the calculated Fe–N–O bond lengths and angles for both DFT methods are in good agreement with experiment, the experimental frequencies are more closely reproduced with the BLYP functional. In fact, the $\nu_{\text{Fe-N(HNO)}}$ and $\nu_{\text{N-O}}$ frequencies from the BLYP/6-311G(2d,2p) calculations differ from the experimental values by $\leq 3\%$. Thus, comparisons to the MbHNO parameters will be based on the results from this method.

One of the most interesting experimental results from MbHNO is the surprisingly high $\nu_{\text{Fe-N(HNO)}}$ frequency of 651 cm^{-1} despite its long Fe–N_{HNO} bond.¹⁰ We have identified a normal mode in the \perp BLYP structure having extensive $\nu_{\text{Fe-N(HNO)}}$ character and whose eigenvector is shown in Figure 3. The frequency of this mode in [FeP(ImH)HNO] is also calculated to be quite high at 631 cm^{-1} and is rather insensitive to whether the HNO and ImH planes are parallel or perpendicular ($\nu_{\text{Fe-N(HNO)}}$ = 634 cm^{-1} for the \parallel and \perp' structures).¹⁶ While there is a small degree of ImH distortion, the character of this mode exhibits significant vertical and slight horizontal N(H) displacement, only slight Fe displacement, and almost no O displacement. These motions amount to significant distortion along the Fe–N_{HNO} bond. The calculated H¹⁵NO isotope shift of 15 cm^{-1} for $\nu_{\text{Fe-N(HNO)}}$ is in perfect agreement with the experimental value of 15 cm^{-1} , suggesting that the calculated normal-mode eigenvector for $\nu_{\text{Fe-N(HNO)}}$ is a reliable mimic of its counterpart in MbHNO.

Despite its long Fe–N_{HNO} bond, the high experimental $\nu_{\text{Fe-N(HNO)}}$ frequency of MbHNO was rationalized by a low effective mass, which was attributed to its small $\angle\text{FeNO}$ of 131°. ¹⁰ While the effective mass does depend on $\angle\text{FeNO}$, it is difficult to rationalize such a high frequency on the smaller $\angle\text{FeNO}$ alone.¹⁷ Unlike Mb{FeNO}⁶ and Mb{FeNO}⁷, MbHNO has a H atom bonded to the coordinated N atom. The BLYP calculation shows an extremely small reduced

mass¹⁸ (μ) of 3.5 amu for $\nu_{\text{Fe-N(HNO)}}$, the value of which is only minimally sensitive to the size of the basis set [μ = 3.7 amu; BLYP/6-31G(d)]. BLYP/6-31G(d) calculations performed on models of Mb{FeNO}⁶ ([FeP(ImH)NO]⁺) and Mb{FeNO}⁷ ([FeP(ImH)NO]) show that μ for the analogous $\nu_{\text{Fe-NO}}$ modes in these models are *both* significantly larger than those for $\nu_{\text{Fe-N(HNO)}}$. The [FeP(ImH)NO]⁺ complex contains a linear FeNO unit for which $\nu_{\text{Fe-NO}}$ has μ = 20.8 amu. However, [FeP(ImH)NO] contains a significantly bent FeNO moiety ($\angle\text{FeNO}$ = 140°) with μ = 15.0 amu for $\nu_{\text{Fe-NO}}$, which is much closer to the linear [FeP(ImH)NO]⁺ value than that of the similarly bent ($\angle\text{FeNO}$ = 132°) [FeP(ImH)HNO] complex. Because the bond strength and effective mass are both intimately related to the energy of a vibrational transition, with the harmonic vibrational frequency being $\propto(k/\mu)^{1/2}$ (k = harmonic force constant and μ = reduced mass), a normal mode in which atoms are displaced along a normal coordinate having a small force constant can have a strikingly high frequency if the reduced mass is also small.

The results of the BLYP/6-311G(2d,2p) calculations predict that isotopic ²HNO substitution will increase the reduced mass of $\nu_{\text{Fe-N(HNO)}}$ by 0.5 AMU to 3.9 AMU, assuming that the force constant remains unchanged by substitution. Barring any distal H-bonding influences, this relatively large change in μ results in a frequency lowering of 39 cm^{-1} in the ²HNO isotopomer, over double that of the H¹⁵NO isotope shift of 15 cm^{-1} , where the same change in molecular mass increases μ by only 0.2 AMU. Hence, we conclude that the large H-atom displacement in this relatively localized $\nu_{\text{Fe-N(HNO)}}$ vibration makes the major contribution to its small reduced mass and, therefore, its high frequency.

To further probe the influence of $\angle\text{FeNO}$ on reduced mass and $\nu_{\text{Fe-N(HNO)}}$, we have performed calculations on the conjugate base of [FeP(ImH)HNO], [FeP(ImH)NO]⁻. The structural parameters for this {FeNO}⁸ complex are listed in Table 1. At the B3LYP/6-31G(d) level of theory, the triplet state ($S = 1$) is found to be lowest in energy. The singlet state ($S = 0$) is higher in energy, but only by 4.5 kJ/mol. Although there are no experimental structure parameters for {FeNO}⁸ porphyrinates having trans ImH ligands, rR data show that the five-coordinate complex, [Fe(TPP)NO]⁻, is low spin and that $\nu_{\text{Fe-NO}}$ and $\nu_{\text{N-O}}$ increase and decrease, respectively, relative to their analogues in the spectrum of [Fe(TPP)NO] ({FeNO}⁷).¹⁹ Whether these changes in the vibrational signature can be directly correlated with changes in the FeNO bond strengths is unclear because the $\angle\text{FeNO}$ angle and bond lengths in the {FeNO}⁸ complex are presently unknown. The results of our DFT calculations on [FeP(ImH)NO]⁻ are consistent with those published for [FeP(NH₃)NO]⁻, wherein the B3LYP/DZVP method predicts a ΔE ($=E_{S=0} - E_{S=1}$) value of 4.6 kJ/mol.⁷ However, the authors of that study stated a preference for the $S = 0$ ground state because a $S = 0$ ground state was reported for an experimental study of a nonheme {FeNO}⁸ complex.⁷ Interestingly, the BLYP/6-

(16) There are other vibrational modes that contain small contributions of Fe–N_{HNO} stretching, specifically the out-of-plane porphyrin distortion at 651 cm^{-1} and the out-of-plane ImH distortion at 660 cm^{-1} .

(17) Linder, D. P.; Rodgers, K. R. *Inorg. Chem.* **2005**, *44*, 1367–1380.

(18) The reduced mass is that from a *Gaussian 03*¹¹ frequency calculation.
(19) Choi, I.-K.; Liu, Y.; Feng, D. W.; Paeng, K.-J.; Ryan, M. D. *Inorg. Chem.* **1991**, *30*, 1832–1839.

31G(d) method only predicts a stable six-coordinate structure with a triplet ground state; on the singlet-state potential energy surface, the trans ImH ligand dissociates to give $[\text{FeP}(\text{NO})]^-$ and ImH. On the basis of these mixed results, the lowest-energy structure of $[\text{FeP}(\text{ImH})\text{NO}]^-$ is not clear. Nevertheless, two general observations are worth noting. First, the Fe–N_{NO} bond in $[\text{Fe}(\text{TPP})\text{NO}]^-$ is likely to be stronger than its counterpart in $[\text{Fe}(\text{TPP})\text{NO}]$, which probably gives rise to the higher $\nu_{\text{Fe}-\text{NO}}$ frequency in $[\text{Fe}(\text{TPP})\text{NO}]^-$. In contrast, on the basis of bond lengths, the Fe–N_{HNO} bonds in $[\text{FeP}(\text{ImH})\text{HNO}]$ and MbHNO appear to be weaker than the Fe–N_{NO} bonds in $[\text{FeP}(\text{ImH})\text{NO}]$ and $\{\text{FeNO}\}^7$ MbNO. Thus, although the computational results do not support a detailed comparison of the $[\text{FeP}(\text{ImH})\text{HNO}]$ and $[\text{FeP}(\text{ImH})\text{NO}]^-$ bonding parameters, it is important to recognize that the reason(s) for increased $\nu_{\text{Fe}-\text{NO}}$ frequency upon formation of $[\text{Fe}(\text{TPP})\text{NO}]^-$ from $[\text{Fe}(\text{TPP})\text{NO}]$ are probably attributable mostly to increased Fe–N bond strength,¹⁹ whereas it is most likely that the $\nu_{\text{Fe}-\text{N}(\text{H})\text{O}}$ frequency for $[\text{FeP}(\text{ImH})\text{HNO}]$ is greater than that of $\nu_{\text{Fe}-\text{NO}}$ for $[\text{FeP}(\text{ImH})\text{NO}]$ because of the low reduced mass of $\nu_{\text{Fe}-\text{N}(\text{H})\text{O}}$.

The BLYP method provides calculated frequencies of all normal modes and can be used for the identification and prediction of vibrational frequencies. The BLYP method shows an Fe–HNO vibrational mode at 1427 (1427.1) cm^{-1} that shifts 5 cm^{-1} to lower frequency upon H^{15}NO substitution. The rR spectrum exhibits a band at 1408 cm^{-1} that undergoes the same 5- cm^{-1} shift upon H^{15}NO isotope substitution.¹⁰ This band remains unassigned but has been speculated to be one of the heme modes (ν_{12} or ν_{29}) whose coupling to the N–O stretching coordinate (vide infra) gives rise to the frequency shift. However, the DFT calculations identify this mode as an in-plane H–N–O bending mode [$\delta_{\text{HNO}}(\text{ip})$] with a small in-plane porphyrin component, as illustrated by the eigenvector in Figure 4D. Other predicted Fe–N(H)–O modes that should be clearly identifiable include an out-of-plane H–N–O bend [$\delta_{\text{HNO}}(\text{oop})$] at 815 cm^{-1} that shifts 11 cm^{-1} to lower energy upon H^{15}NO substitution and an Fe–N(H)–O scissoring mode at 448 cm^{-1} that shifts 2 cm^{-1} to lower frequency upon H^{15}NO substitution and only 1 cm^{-1} for ^2HNO substitution.

An interesting insight provided by both DFT methods is that the $R_{\text{H}-\text{NO}}$ decreases upon HNO binding to iron. This result may be experimentally observable, as described below, and is consistent with the π acidity seen for HNO in other transition-metal complexes.^{20a} In accordance with the shortened bonds, a $[\text{FeP}(\text{ImH})\text{H}-\text{NO}]$ stretch, $\nu_{\text{N}-\text{H}}$, is calculated at 3008 cm^{-1} (cf. 2625 cm^{-1} calculated for free HNO) with downshifts of 6 and 808 cm^{-1} upon H^{15}NO and ^2HNO substitution, respectively.

Both experimental¹⁰ and DFT results reveal increased $R_{\text{HN}-\text{O}}$ upon formation of the Fe–N(H)–O complex. On the basis of its 30- cm^{-1} downshift upon H^{15}NO substitution, the Raman band at 1385 cm^{-1} has been assigned to $\nu_{\text{N}-\text{O}}$.¹⁰

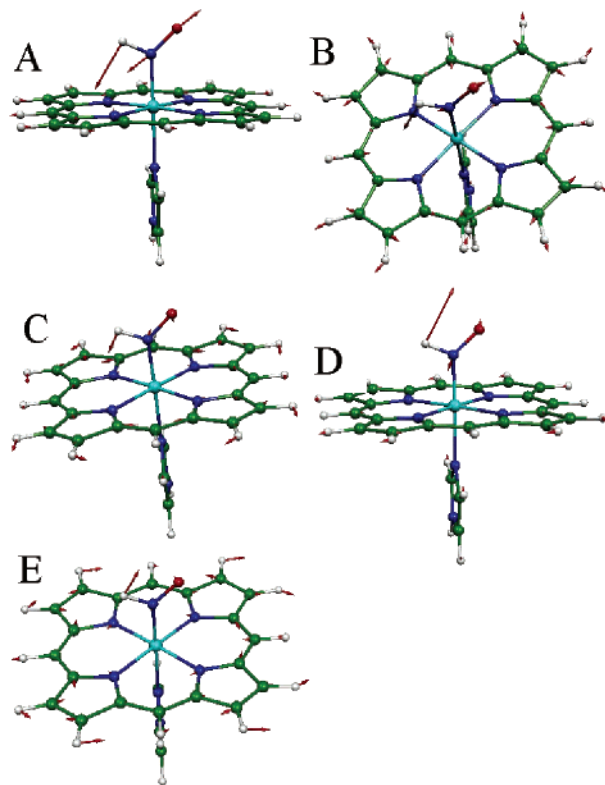


Figure 4. Eigenvectors for vibrational modes of $[\text{FeP}(\text{ImH})\text{HNO}]$ obtained at the BLYP/6-311G(2d,2p) level of theory: (A) 1416.3 ($\nu_{\text{N}-\text{O}}$), (B) 1419.2, (C) 1426.8, (D) 1427.1 [$\delta_{\text{HNO}}(\text{ip})$], and (E) 1429.5 cm^{-1} .

Consistent with its longer HN–O bond, this energy is 178 cm^{-1} lower than that of free HNO, for which $\nu_{\text{N}-\text{O}}$ occurs at 1563 cm^{-1} .^{4,15} The BLYP/6-311G(2d,2p) method predicts $\nu_{\text{N}-\text{O}}$ at 1416 cm^{-1} (a H^{15}NO shift of -24 cm^{-1}) for $[\text{FeP}(\text{ImH})\text{NO}]$ (Figure 4A). The reduction of 143 cm^{-1} for $\nu_{\text{N}-\text{O}}$ from its calculated value of 1559 cm^{-1} in free HNO is similar in magnitude to the 178 cm^{-1} seen experimentally for MbHNO. It has been speculated that, for MbHNO, $\nu_{\text{N}-\text{O}}$ couples to the porphyrin π^* marker band, ν_4 , at 1374 cm^{-1} and the unassigned band at 1408 cm^{-1} .¹⁰ The BLYP calculations reveal that $\nu_{\text{N}-\text{O}}$ does indeed have a small degree of in-plane porphyrin character. Moreover, the primarily porphyrin modes at 1419.2, 1426.8, and 1429.5 cm^{-1} (parts B, C, and E of Figure 4) all have $\delta_{\text{HNO}}(\text{ip})$ character. Additionally, the 1419.2 cm^{-1} mode has $\nu_{\text{N}-\text{O}}$ character. Hence, there are a number of closely spaced normal modes that, by virtue of the proximity between the natural porphyrin, $\nu_{\text{HN}-\text{O}}$, and δ_{HNO} frequencies, exhibit displacement along porphyrin and HNO coordinates.

Heme–HNO complexes are implicated in bacterial and fungal heme-mediated reduction of NO. Although there is no evidence that the bacterial NO reductase mechanism involves a $\{\text{FeNO}\}^6$ heme,²¹ there is evidence to suggest that the mechanisms of cytochrome *c* nitrite reductase (cyt *c* NiR)⁷ and cytochrome P450 NO reductase (P450_{NOR})²² do. Thus, it is of interest to compare the Fe–HNO bonding parameters with those of the $\{\text{FeNO}\}^6$ complexes from which NO reduction originates. Such comparisons have been made

(20) (a) Southern, J. S.; Green, M. T.; Hillhouse, G. L.; Guzei, I. A.; Rheingold, A. L. *Inorg. Chem.* **2001**, *40*, 6039–6046. (b) Melenkivitz, R.; Southern, J. S.; Hillhouse, G. L.; Concolino, T. E.; Liable-Sands, L. M.; Rheingold, A. L. *J. Am. Chem. Soc.* **2002**, *124*, 12068–12069.

(21) Zumft, W. G. *J. Inorg. Biochem.* **2005**, *99*, 194–215.

(22) Silaghi-Dumitrescu, R. *Eur. J. Inorg. Chem.* **2003**, 1048–1052.

Table 2. Comparison of the Fe–N and N–O Bond Lengths in {FeNO}⁶ and Fe–HNO Porphyrinates Having Different Proximal Ligands To Mimic the Indicated Proteins and Enzymes

complex	$R_{\text{Fe-N}} (\text{\AA})$	$R_{\text{N-O}} (\text{\AA})$	$\angle\text{FeNO} (\text{deg})$	$R_{\text{Fe-L}} (\text{\AA})$	protein/enzyme	comments
[FeP(ImH)NO] ⁺	1.639	1.136	179.7	2.024	myoglobin	ref 17
[FeP(ImH)HNO]	1.809	1.224	132	2.091		this work, Figure 1
[FeP(NH ₃)NO] ⁺	1.630	nr ^a	“linear”	2.034	cyt <i>c</i> NiR	ref 7
[FeP(NH ₃)HNO]	1.782	1.23	131	2.120		ref 7
[FeP(SCH ₃)NO]	1.67	1.18	163	2.30	cyt P450 _{NOR}	ref 22
[FeP(SCH ₃)HNO] ⁻	1.81	1.26	135	2.37		ref 22

^a nr: not reported.

computationally by applying DFT-based geometry optimization methods to models of the P450_{NOR}²² and cyt *c* NiR⁷ heme sites. The trans ligands in these models were chosen to mimic the proximal thiolate and amine ligand fields of the respective enzymes. Although there are no experimental data on the HNO complexes of these enzymes, the Fe–N and N–O bonds were calculated to be longer in the Fe–HNO model complexes than in the analogous {FeNO}⁶ porphyrinates. These results are compiled in Table 2. Lengthening of the Fe–N and N–O bonds in the FeHNO complex relative to the corresponding {FeNO}⁶ species reported herein is similar to those reported for models of P450_{NOR}²² and cyt *c* NiR⁷ (Table 2). Among the three models compared in Table 2, that for P450_{NOR} appears shortened to a slightly lesser extent. Although the calculated bond lengths of the three model systems in Table 2 cannot be directly compared because of differences in DFT functionals and basis sets, the smaller diminution of bond lengths upon Fe–HNO formation of a trans thiolate ligand may not be surprising. We have shown that axial coordination of {FeNO}⁶ porphyrinate by anionic imidazolate¹⁷ or thiolate²³ ligands causes off-axis distortion of the {FeNO}⁶ moiety and concomitant weakening of both the Fe–N_{NO} and N–O bonds relative to the corresponding complexes having neutral imidazole or thiol ligands. This difference in {FeNO}⁶ bonding is attributed to the increased FeNO antibonding character of the highest occupied molecular orbitals for the complexes containing anionic trans axial ligands. Thus, in the comparison of the P450_{NOR} models in Table 2, it should be considered that the lengthening effect is diminished because the {FeNO}⁶ bonds are probably longer to begin with. Nevertheless, consistent with the expectation for NO reduction, the Fe–N and N–O bonds appear to lengthen upon formation of the heme–HNO complex, regardless of the identity of the proximal ligand. The similarity of the calculated FeHNO bonding parameters reported here with

those determined experimentally for MbHNO suggests that previously calculated bonding parameters for models of NO-reducing enzymes provide accurate views of the putative heme–HNO intermediates in the corresponding mechanisms.

Conclusions

These DFT calculations provide insight into the interplay among Fe–N(H)–O structure, electronic properties, and vibrational dynamics in recently discovered HNO complexes of metalloporphyrinates. The results are consistent with an N(H)-bound [FeP(ImH)HNO] singlet ground state having a strikingly high $\nu_{\text{Fe-N(HNO)}}$ frequency, which is attributed to H_{HNO} atom motion and its diminutive influence on the effective mass. This example, albeit somewhat extreme, serves as a reminder that comparison of vibrational frequencies as indicators of relative bond strengths in molecules of differing composition or connectivity should be approached with caution. Finally, the relative orientations of the HNO and ImH ligands does not appear to have a major influence on either the porphyrin planarity or the energy of the complex. Moreover, the barrier for interconversion between the parallel and perpendicular orientations is probably only a few kilojoules per mole. As expected for the reduction of the FeNO moiety, the Fe–N and N–O bond distances both increase upon formation of the FeHNO complex.

Acknowledgment. The authors thank Dr. Michael Page for helpful discussions and the Center for High Performance Computing (CHPC) at NDSU, where calculations were performed. Financial support from the USDA (Grant ND05299), Hermann Frasch Foundation (Grant 446-HF97), and NCRR (Grant P20 RR15566) is also gratefully acknowledged.

Supporting Information Available: Figure of all of the filled Kohn–Sham orbitals having Fe–L_{axial} character for the \perp and \parallel conformers. This material is available free of charge via the Internet at <http://pubs.acs.org>.

(23) Linder, D. P.; Rodgers, K. R., submitted for publication.